

Quantum Ising Heat Engines: A mean field study¹

Muktish Acharyya^{a,*} and Bikas K. Chakrabarti^{b,†}

^a*Department of Physics, Presidency University, Kolkata-700073, India*

^b*Saha Institute of Nuclear Physics, Kolkata 700064, India*

*muktish.physics@presiuniv.ac.in

†bikask.chakrabarti@saha.ac.in

Abstract: We have studied the efficiencies of both classical and quantum heat engines using an Ising model as working fluid and the mean field equation for its non-equilibrium dynamics, formulated earlier [1, 2] to study the dynamical hysteresis and the dynamical phase transitions in the quantum Ising ferromagnets. We studied numerically the Ising magnet's nonintegrable coupled nonlinear first order differential equations of motion for a four stroke heat engine and compared the efficiencies in both classical and quantum limits using the quasi-static approximation. In both the pure classical and pure quantum cases, the numerically calculated efficiencies are much less than the corresponding Carnot values. Our analytical formulations of the efficiencies (both in pure classical as well as in pure quantum Ising heat engines) are found to agree well with the numerical estimates. Such formulations also indicate increased efficiency for the mixed case of a transverse field driven Ising engine in presence of nonzero longitudinal field. We also numerically checked and found that the efficiency of such a (mixed) quantum Ising heat engine can indeed have much higher efficiency for appropriate values of the transverse and longitudinal fields.

Keywords: Quantum heat engine, Ising model in transverse field, Generalized mean field equation of dynamics, Runge-Kutta method, Engine efficiency

¹Dedicated to the loving memory of Prof. Amit Dutta, Indian Institute of Technology, Kanpur

I. Introduction

Starting from the earliest proposal for a quantum heat engine [3] (using a three level Maser) and the first proposal for the quantum version of thermodynamics, defining heat and work in the quantum regime [4], successive developments [5–8], and also the timely reviews [9–12] led to the recent resurgence of theoretical model studies for quantum heat engines and their efficiencies in comparison with almost two-century old and thoroughly established classical heat engines which have since become a part of our every-day life. These engines typically consist of a ‘heat reservoir’ (at high temperature), a heat sink (at lower temperature) and a ‘working fluid’, which facilitates the (irreversible) process of extracting work from heat. Classical heat engines and refrigerators being the major source of mechanical energy or work in industry as well as in household, the need for miniaturization of such heat engines also led to the quest for quantum heat engines, where the working fluid will be a quantum system (likely many-body).

In this paper we consider a quantum heat engine, where the working fluid is a quantum Ising magnet (more specifically, Ising model in transverse field; see e.g., [13, 14]), for which the dynamics of Ising spins (average magnetization) follow a mean field equation, developed in connection with the study of quantum hysteresis [1, 2]. These dynamical equations for similar open quantum systems have been compared with other formulations (see e.g., [15] and references therein) and also discussed in connection with dynamic simulation of materials for near-term quantum computers (see e.g., [16, 17]). It may be mentioned that some analytical results for a quantum heat engine, using a one dimensional Transverse Ising system (as working fluid), has already been reported [18] and the work efficiency was seen to increase near the critical point. However, their results are extremely limited due to the one dimensional constraint of the spin system considered. Our working fluid system has in general higher dimensional quantum many-body (non-integrable) feature, though studied here using mean field dynamics for the engine strokes, which is not Otto type. In the nonintegrable system considered here, we are essentially solving the coupled nonlinear differential equation [1, 2]. Apart from changing the temperature, we have two distinct strokes (first and the third strokes), where the field is changing. In these strokes, the temperature (a parameter in the equations of magnetisation dynamics) is kept fixed. These are basically the “isothermal” strokes of our quantum heat engine and the working fluid system (here quantum Ising magnet) is allowed to exchange heats with the source or sink. The other two strokes where temperature changes are assumed to be “adiabatic”. Our numerical study here does not indicate any significant dependence of the engine efficiency with the ratio of durations of these “adiabatic” and “isothermal” strokes. Though the efficiency of pure quantum Ising engines are seen to be quite small, the engine efficiency of such quantum Ising engine can approach the Carnot value for optimal presence of longitudinal field. This is consistent with the observation [18] in one dimensional quantum Ising heat engine. We believe, though a mean field study, this many-body quantum heat engines with higher dimensional working fluid systems can be useful for wider applicability and comparisons, as in many nointegrable condensed matter dynamical systems studied in different contexts.

II. Mean field equation and numerical solution

The Hamiltonian of Ising ferromagnet in presence of both transverse and longitudinal external magnetic field is represented as

$$\mathcal{H} = - \sum_{ij} J_{ij} \sigma_i^z \sigma_j^z - h \sum_i \sigma_i^z - \gamma \sum_i \sigma_i^x. \quad (1)$$

Here, $\vec{\sigma}$ denotes the Pauli spin matrix, h and γ are the external longitudinal and transverse fields

respectively, J_{ij} is the ferromagnetic interaction strength between the spins placed at i -th and j -th sites. It may be noted here that due to the presence of transverse field (noncommuting component of the Hamiltonian with σ_z), the quantum nontrivial dynamics of σ^z arises from standard Heisenberg equation of motion. However, one can expect a simplified form of the dynamical evolution in the mean field approximation [1, 2].

The mean field Hamiltonian can be written as

$$\mathcal{H} \cong \sum \vec{h}_{eff} \cdot \vec{\sigma}, \quad (2)$$

with the effective magnetic field

$$\vec{h}_{eff} \cong (m_z + h)\hat{z} + \gamma\hat{x}, \quad (3)$$

where $m_z = \langle \sigma^z \rangle$, the z -component of average magnetisation. The magnitude of the effective magnetic field is

$$|\vec{h}_{eff}| \cong \sqrt{(m_z + h)^2 + \gamma^2}. \quad (4)$$

The generalized mean field dynamics of the Ising ferromagnet in presence of both longitudinal and transverse field, extending the classical Suzuki-Kubo formalism [19], can be represented [1] by the following differential equation:

$$\tau \frac{d\vec{m}}{dt} = -\vec{m} + \tanh\left(\frac{|h_{eff}|}{T}\right) \frac{\vec{h}}{|h_{eff}|}. \quad (5)$$

The above vector differential equation is basically first order nonlinear coupled differential equations of $m_x (= \langle \sigma^x \rangle)$ and $m_z (= \langle \sigma^z \rangle)$. They can be written as

$$\tau \frac{dm_x}{dt} = -m_x + \tanh\left(\frac{|h_{eff}|}{T}\right) \frac{\gamma}{|h_{eff}|} \quad (6)$$

and

$$\tau \frac{dm_z}{dt} = -m_z + \tanh\left(\frac{|h_{eff}|}{T}\right) \frac{(m_z + h)}{|h_{eff}|}. \quad (7)$$

For the classical case ($\gamma = 0$), in the static limit ($dm_z/dt = 0$), eqn. (7) gives the Bragg-William form of the mean field Ising equation of state (see e. g., [20, 21]), while in the dynamic case extensive studies (see e.g., [22, 23]) of dynamic hysteresis and other phenomena in classical Ising model have been studied. For the quantum case (with $h = 0$) the static limit ($dm_x/dt = 0$) of eqn. (6) had been utilized extensively to model the order-disorder transition behavior in ferro-electric materials [24] (see also [13]).

These two coupled first order nonlinear differential equations have been solved by fourth order Runge-Kutta method [25] with time step $dt = 10^{-2}$, so that the order of the local error is significantly small. The initial conditions are $m_z(t = 0) = 1.0$ and $m_x(t = 0) = 0.0$. We have calculated the instantaneous components of the magnetization, i.e., $m_x(t)$ and $m_z(t)$. The instantaneous internal energy ($U = m_z^2 + hm_z + \gamma m_x$) of the system has also been calculated using eqns. (6) and (7) for different drives.

III. Four stroke Classical and quantum Ising heat engines

A schematic diagram for the four strokes of a complete cycle for both classical and quantum heat engines are shown in Fig. 1. The details of the four strokes of any cycle of the Ising engine,

both classical and quantum, are given in the figure caption. In the following, we present our results separately for the two cases of this mean field Ising heat engine, namely (a) classical (where the transverse field $\gamma = 0$) and (b) quantum (where the longitudinal field $h = 0$).

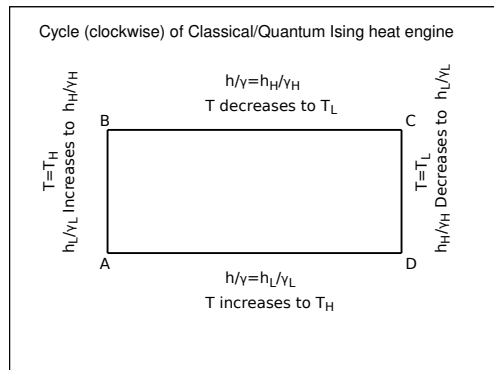


Figure 1: A schematic diagram of the cycle of engine. This starts from A and returns to A after a clockwise rotation. A schematic diagram of the for strokes AB, BC, CD and DA of the engines. For classical Ising heat engine, stroke AB corresponds to fixed high temperature $T = T_H$ while the longitudinal field h changes from h_L to h_H , stroke BC corresponds to fixed high field $h = h_H$ while the temperature T changes from T_H to T_L , stroke CD corresponds to fixed low temperature $T = T_L$ while the longitudinal field h changes from h_H to h_L , and finally the fourth stroke DA corresponds to fixed field $h = h_L$ while the temperature T changes from T_L to T_H . For the quantum Ising heat engine, the first stroke AB corresponds to fixed high temperature $T = T_H$ while the transverse field γ changes from γ_L to γ_H , stroke BC corresponds to fixed high transverse field $\gamma = \gamma_H$ while the temperature T changes from T_H to T_L , stroke CD corresponds to fixed low temperature $T = T_L$ while the transverse field γ changes from γ_H to γ_L , and finally the fourth stroke DA corresponds to fixed transverse field $\gamma = \gamma_L$ while the temperature T changes from T_L to T_H .

A complete cycle of the engine (shown in Fig. 1) consists of the following four strokes (each having equal duration, much higher than microscopic relaxation time τ):

- (i) A→B: Field (longitudinal h , in classical case or transverse field γ , in quantum case) increases linearly with time from a low value, h_L or γ_L , to a high value, h_H or γ_H) at a constant high temperature T_H of the heat bath. Heat is absorbed by the engine during this stroke. This is an isothermal stroke. The system is absorbing the heat from the heat source. The internal energy of the system increases in this stroke. As in the Carnot engine, this absorbed heat pushes the piston outward and the engine produces mechanical work.
- (ii) B→C: Thermalization with the cold bath(heat sink) at temperature T_L . The field remains fixed but the temperature of the system decreases linearly from T_H to T_L .
- (iii) C→D: The field decreases linearly from the high value (h_H or γ_H) to the low value (h_L or γ_L). Temperature remains fixed at T_L . The heat is being released in this stroke. This is also an isothermal stroke. The system is releasing heat to the heat sink. The internal energy is found to decrease in this stroke. In the Carnot cycle of this isothermal stroke (at lower temperature) the piston is being pulled inward by the engine (by utilizing a part of the mechanical work produced by the engine).
- (iv) D→E: The field remains fixed (at h_L or γ_L) and the temperature increases linearly from T_L to T_H .

The system returns to its original (initial) state after the completion of a cycle. Hence, the thermodynamic state of the system denoted by A and that denoted by E are same in all respect. A schematic diagram of the cycle is shown in Fig. 1.

The change in the internal energy would provide the heat absorbed by the system and heat released by the system. Here, the heat will be absorbed by the system in the first stroke (A→B). The heat absorbed $E_{absorbed} = U(B) - U(A)$, where $U(A)$ and $U(B)$ represents the internal energy at state-A and that of state-B respectively. The heat is released in the third stroke (C→D) by the system. The heat released is $E_{released} = |U(D) - U(C)|$ (to keep it positive). So, the efficiency is $\eta = (E_{absorbed} - E_{released})/E_{absorbed}$.

In the numerical study and thermodynamic estimates, we have discarded many transient cycles (typically about 49 such cycles) and then calculated the thermodynamic quantities in a stable cycle (typically on 50th cycle). Each cycle consists of four strokes and each stroke consists of 10000dt elapsed time of the differential equation. The maximum value of the relaxation time τ used here is 0.2 (much less than 10000dt = 100 here) to maintain the quasi static limit of the thermodynamic working speed of the engines.

IV. Numerical solutions of mean field equations and estimates of internal energy and engine efficiency in quasi-equilibrium approximation

(IV.1) Classical case:

In the calculation of classical efficiency, η_C , we have used $T_L = 0.05$ and $T_H = 1.05$ (slightly above the critical temperature of ferro-para transition). The transverse field $\gamma = 0.0$ (always). The longitudinal field varies between $h_L = 0$ and h_H . The instantaneous components of the magnetisations (m_x and m_z) are depicted in Fig. 2.

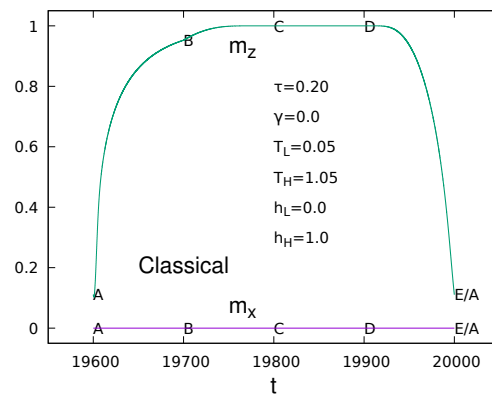


Figure 2: Numerical solutions of eqns. (6) and (7) for the components (m_x and m_z) of the magnetization, plotted against time (t) over a full steady state cycle for the classical Ising heat engine ($\gamma = 0$).

In the classical calculations ($\gamma = 0$) the transverse components of the magnetisation, m_x will always remain zero. The dynamics will be represented by m_z only. The instantaneous internal energy ($U_C = m_z^2 + m_z h$) are shown in Fig. 3.

We have studied the efficiency η_C as function of h_H for two different values of the microscopic relaxation time τ . The values of τ are kept small to ensure the quasi-static process is maintained in classical thermodynamic engines. The efficiency has been calculated from the change in the internal energy. The efficiency is studied as a function of the h_H . In our numerical simulation,

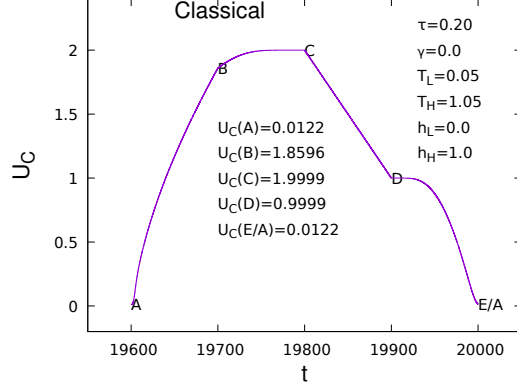


Figure 3: The numerically estimated internal energy ($U_C = m_z^2 + hm_z$) of the working fluid (Ising magnet), plotted against time (t) over a full steady state cycle for the classical Ising heat engine ($\gamma = 0$).

we have calculated the efficiency from a steady cycle. We have discarded 49 number of initial transient cycles. The 50th steady cycle has been used to calculate the efficiency. Each cycle consists of four strokes. Each strokes consists of 10000 times steps (in the unit of dt). We have used $dt = 0.01$. The results are shown in Fig. 4. The numerical results are in good agreement with the theoretical prediction ($\eta_c = 1/[1 + h_H]$).

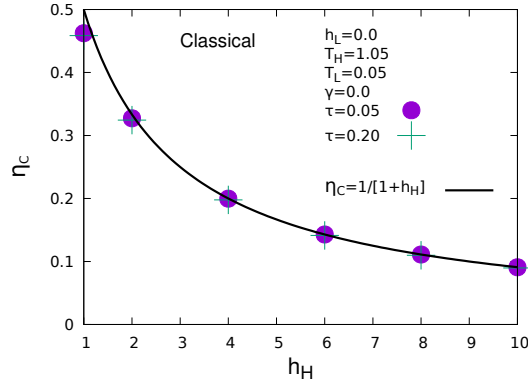


Figure 4: The efficiency η_C in the case of absence of transverse field ($\gamma = 0$) is plotted against the longitudinal field h_H . Two different symbols represent two different values of the microscopic relaxation time τ . The solid line represents the analytical result ($\eta_C = R_c/[1 + h_H]$), where $R_c = 1$.

(IV.1a) Theoretical estimate of classical efficiency η_C :

We estimate η_C for the case where $T_L = 0, T_H = 1_+, h_L = 0$ and $h_H > 1$. For the classical case the energy $U_C = m_z^2 + hm_z$ and we get (see Fig. 1), using equilibrium results for the above parameter values, $U_C(A) = 0, U_C(B) = 1 + h_H, U_C(C) = 1 + h_H$ and $U_C(D) = 1$. This gives $U_C(B) - U_C(A) = 1 + h_H$ for the heat energy taken and $U_C(C) - U_C(D) = 1$ for the heat energy released by the classical Ising engine, giving

$$\eta_C = \frac{[(U_C(B) - U_C(A)) - (U_C(C) - U_C(D))]}{[U_C(B) - U_C(A)]} = \frac{R_C}{[1 + h_H]}, \quad (8)$$

with an adjustable parameter R_C of order m_z^2 for the dynamic case considered in the simulations.

In Fig. 4 we plot the numerical estimates of the classical Ising heat engine efficiency (for two values of the microscopic relaxation time τ in eqn. (5); here of course for numerical stability we kept $T_L = 0.05$). The results agree fairly well with the above-mentioned theoretical estimate of η_C with $R_C = 1.0$.

(IV.1b) Classical efficiency for nonuniform stroke distribution

In order to check if shorter “adiabatic” stroke duration (L_{Adia} for strokes B→C and D→A in Fig. 1) compared to the duration (L_{Iso}) of “Isothermal” strokes (A→B and C→D in Fig. 1)) affect the classical Ising engine efficiency, we studied numerically for two cases ($L_{Iso} = 2L_{Adia}$ and $L_{Iso} = 4L_{Adia}$), shown in Fig. 5. As may be seen, we could not detect any significant change.

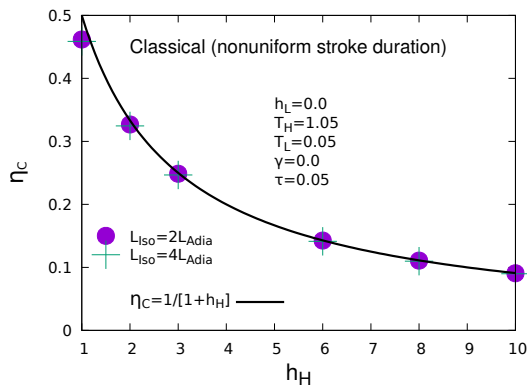


Figure 5: Classical efficiency η_C , plotted against the longitudinal field h_H for two different fractions of the “adiabatic” stroke duration L_{Adia}/L_{Iso} , compared to the “isothermal” stroke duration (represented by two different symbols). The solid line again represents the analytical result ($\eta_C = R_c/[1 + h_H]$), with $R_c = 1$, derived above.

(IV.2) Quantum case:

Our study has been extended in the presence of transverse magnetic field γ in the absence of any strong longitudinal field (using $h = 0_+$) to investigate the quantum (transverse Ising ferromagnet) effects in the mean field approximation. In this case, the transverse magnetisation ($m_x \neq 0$) plays the crucial role in determining the efficiency. Here also, like the classical case, each cycle (four-stroke) consists of 40000 time units (in the unit of $dt = 0.01$). Initial 49 number of transient cycles are discarded to achieve steady cycle. The quantities are calculated from 50th steady cycle. The ranges of the temperatures are set as used in the case of classical study. The transverse field operates within range $\gamma_L = 0.5$ and $\gamma_H = 10$. We have studied the efficiency η_Q as function of γ_H keeping $\gamma_L = 0.5$ fixed. The time dependence of the components of the magnetizations (m_x and m_z) are shown in Fig. 6. It may be mentioned here that, accurately speaking, the longitudinal magnetization m_z has, for $h = 0_+$, a little growth with the drive of γ_H up to the dynamic critical point value near unity, missed because of some subtle instabilities.

The internal energy of the system U_Q has been calculated using the mean field approximation $U_Q \cong m_z(m_z + h) + m_x\gamma$ assuming a tiny longitudinal field $h = 0_+$. The instantaneous energy U_Q has been shown in Fig. 7. Finally, the efficiency, η_Q has been studied and shown in Fig. 8 as function of γ_H . Unlike the classical case, here, the efficiency shows a nonmonotonic variation. The data are fitted (see eqn. (9)) with a function $\eta_Q = [R_Q\gamma_{High}^2]/[1 + R'_Q\gamma_{high}^3]$, where $R_Q = 1/12$ and $R'_Q = 1/4$. This shows good agreement with analytical prediction.

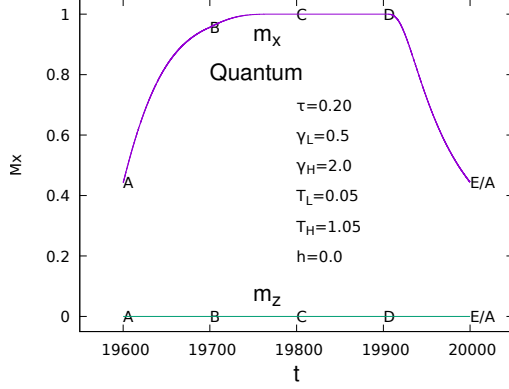


Figure 6: Numerical solutions of eqns. (6) and (7) for the components (m_x and m_z) of the magnetization, plotted against time (t) over a full steady state cycle for the quantum Ising heat engine (in presence of transverse field γ and in absence of the longitudinal field; $h = 0$).

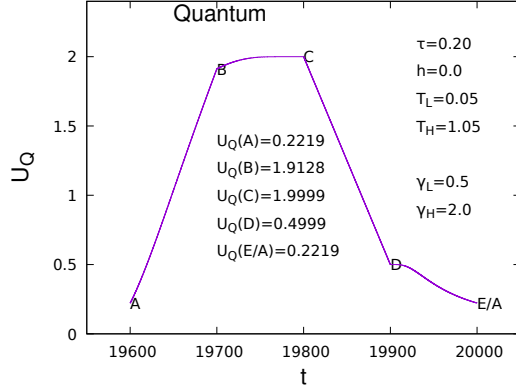


Figure 7: Numerically estimated internal energy ($U_Q = m_z^2 + \gamma m_x$) of the working fluid (quantum Ising magnet), plotted against time (t) over a full steady state cycle (for longitudinal field $h = 0$, and in the presence of transverse field γ).

(IV.2a) Theoretical estimate of efficiency η_Q :

We estimate η_Q theoretically for the case where $T_L = 0, T_H = 1_+, \gamma_L = 0$ and $\gamma_H \gg 1$. For this quantum case, in order to see the competition between the classical or longitudinal order (m_z) explicitly with the quantum or transverse order (m_x) of the Ising magnetization, we consider a tiny longitudinal field ($h = 0_+$) for calculating the internal energy $U_Q = m_z^2 + \gamma m_x$. We then get (see Fig. 1), using the quasi-equilibrium results for the above parameter values, $U_Q(A) = 0, U_Q(B) = U_Q(C) \simeq 1/\gamma_H^2 + \gamma_H$ (as $m_z^2 \simeq 1/\gamma_H^2$ from eqn. (7), $m_x \simeq 1 - m_z^2/2\gamma_H^2$ from eqn. (6), for $\gamma_H \gg 1$ and the constraint $m_x^2 + m_z^2 = \tanh^2(|h_{eff}|/T) \simeq 1$), and $U_C(D) = 1$

$$\eta_Q = \frac{[(U_Q(B) - U_Q(A)) - (U_Q(C) - U_Q(D))]}{[(U_Q(B) - U_Q(A))]} = \frac{R_Q}{[\frac{1}{\gamma_H^2} + R'_Q \gamma_H]}, \quad (9)$$

with two adjustable parameters R_Q, R'_Q both less than unity as they are of order m_z^2 for the dynamic case considered in the simulations.

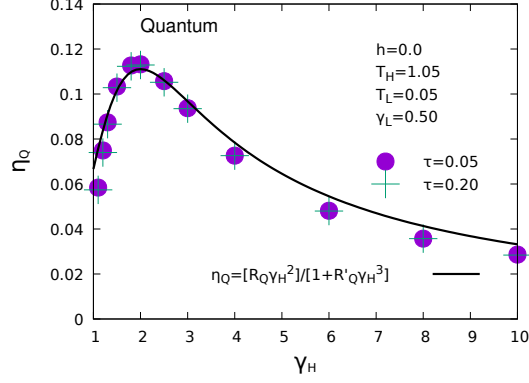


Figure 8: The efficiency η_Q of the quantum Ising heat engine is plotted against the peak value (γ_H) of the transverse field or quantum tunneling probability in the Hamiltonian (1). Here, $h = 0_+$ and $\gamma_L = 0.5$. Two different symbols represent two different values of the microscopic relaxation time τ . The solid line represents the best fit to eqn. (9): $\eta_Q = [R_Q \gamma_H^2] / [1 + R'_Q \gamma_H^3]$, where $R_Q = 1/12$ and $R'_Q = 1/4$. Note that $\gamma_H = 1$ corresponds to the (equilibrium) quantum critical point (zero temperature) of the mean field system.

In Fig. 8 we plot the numerical estimates of the quantum Ising heat engine efficiency (again for two values of the microscopic relaxation time τ in eqn. (5); here also for numerical stability we kept $T_L = 0.05$). It agrees fairly well with the theoretical estimate (eqn. (9)) with the phenomenological fit values of the parameters $R_Q = 1/12$ and $R'_Q = 1/4$.

(IV.2b) Quantum efficiency for nonuniform stroke distribution

Again to check if shorter “adiabatic” stroke duration (L_{Adia} for strokes B→C and D→A in Fig. 1) compared to the duration (L_{Iso}) of “Isothermal” strokes (A→B and C→D in Fig. 1) affect the quantum Ising engine efficiency, we studied numerically two cases ($L_{Iso} = 2L_{Adia}$ and $L_{Iso} = 4L_{Adia}$), shown in Fig. 9. In this case also, we could not detect any significant change of the quantum efficiency.

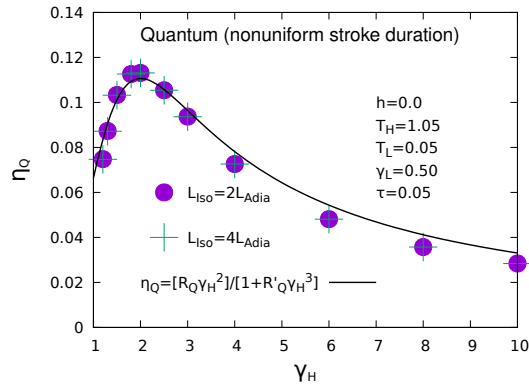


Figure 9: Quantum Ising efficiency η_Q , plotted against transverse field γ_H for two different fractions of the “adiabatic” stroke duration L_{Adia}/L_{Iso} , compared to the “isothermal” stroke duration (represented by two different symbols). The solid line again represents the analytical result (eqn. (9)) with identical parameter values as in Fig. 8.

(IV.2c) Quantum case with nonzero longitudinal field:

We have seen very low values of pure quantum Ising engine efficiency, discussed above and shown in Fig. 8. The theoretical estimate of efficiency η_Q , discussed in section (IV.2b) above indicates that the quantum efficiency can be significantly increased in presence of nonzero longitudinal magnetic field (h). This was also suggested by the observation [18] of increased efficiency in one dimensional quantum Ising heat engine at zero temperature. In Fig. 10, we show the numerically estimated efficiency η_Q (as function of γ_H , of the engine with the same parameters as in Fig. 7, with $h = 0.1, 0.5$ and 1.5 . Fig. 11 shows the variations of η_Q at transverse field terminal value $\gamma_H = 1.1$ and 4.0 , against the longitudinal field h from Fig. 10.

The observed good fit of these data to eqn. (9), with γ_H replaced by h , again confirms its validity with the values of $R_Q(\gamma_H)$ as well as of $R'_Q(\gamma_H)$. It also indicated that the maximum quantum heat engine efficiency $\eta_Q \simeq 0.78$ at $\gamma_H \simeq 1.10$ with $h \simeq 0.15$). Whereas the limiting Carnot value $(1 - T_L/T_H)$ is around 0.95.

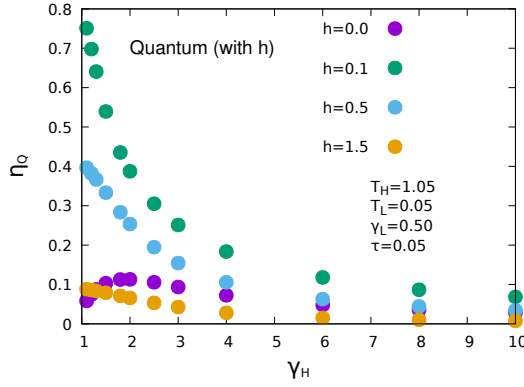


Figure 10: Quantum Ising engine efficiency η_Q against the transverse field value γ_H for different longitudinal field (h) values.

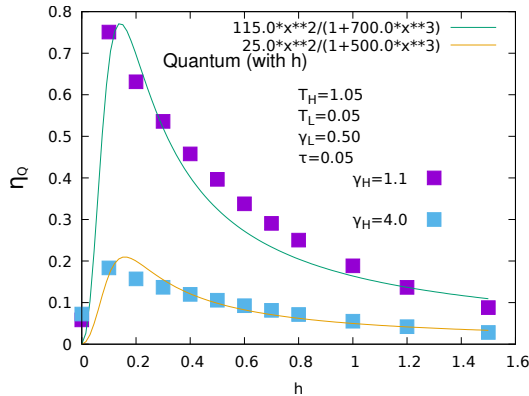


Figure 11: Plot of quantum Ising efficiency η_Q vs. longitudinal field strength (h) for two chosen values of transverse field γ_H . The observed fit of these data to eqn. (9), with γ_H replaced by h , indicates that the maximum value of efficiency of such quantum Ising heat engine (having $T_H = 1.05$ and $T_L = 0.05$) becomes $\eta_Q \simeq 0.78$ at $\gamma_H \simeq 1.10$ with $h \simeq 0.15$. Whereas, the Carnot efficiency $(1 - T_L/T_H)$ is approximately equal to 0.95.

V. Summary and discussions

We studied here numerically (using Runge-Kutta method) the generalized mean field dynamical equations of the longitudinal (m_z) and transverse (m_x) components of the magnetization, using a generalized form ([1], see e.g., [2, 13] for details) of the Suzuki-Kubo formalism [19] for the classical Ising magnet, for a four stroke (open and irreversible) quantum Ising heat engine (see Fig.1). We also estimated, using quasi-equilibrium approximation, the efficiencies of the heat engines in both classical and quantum limits (see eqns. (8) and (9)). We find that their generic forms agree well (see Figs. 4 and 8) with our numerical estimates. We tried to check if shorter “adiabatic” stroke duration (L_{Adia} for strokes B→C and D→A in Fig. 1), compared to the duration (L_{Iso}) of “Isothermal” strokes (A→B and C→D in Fig. 1), would increase the classical or quantum Ising engine efficiencies. Our numerical studies, for two cases ($L_{Iso} = 2L_{Adia}$ and $L_{Iso} = 4L_{Adia}$), shown in Fig. 5 (classical case) and Fig.9 (quantum case) did not indicate any significant change of quantum Ising engine efficiencies. In both cases, the efficiencies are much less than the corresponding Carnot values ($\eta_{Carnot} = 1 - T_L/T_H$) for temperatures $T_H = 1.05$ of the heat reservoir and $T_L = 0.05$ of the heat sink in the classical and quantum engines considered here. For quantum Ising heat engine, however, the efficiency η_Q has been found to increase significantly (see section IV.2c) in presence of optimal value of the longitudinal field. This is also consistent with the observation [18] of increased efficiency in presence of optimal value of h in one dimensional ($T = 0$) quantum Ising engine. As may be seen from Fig. 11, the best fit the analytical form (9) of the quantum Ising heat engine efficiency (with γ_H replaced by h in the equation and using γ_H dependent fitting parameters R_Q and R'_Q) becomes maximum ($\eta_Q \simeq 0.78$) at $\gamma_H \simeq 1.10$ with $h \simeq 0.15$. We also note, similar to the observation of a shift from the equilibrium quantum critical point for the maximum efficiency point in the one dimensional quantum Ising heat engine [18], the efficiency of such mean field quantum Ising heat engine also becomes maximum (see Fig. 8) above the equilibrium quantum critical point.

It may be noted here, that the cycles described for such a quantum Ising heat engine (studied by solving the coupled nonlinear differential equations) are different from those of the Otto-like cycles for integrable one dimensional Ising engine considered earlier [18]. We have calculated the efficiency just from the amounts of heat absorbed and released by the engine. The first stroke (A→B, isothermal and field increasing) provides the heat absorbed from the heat reservoir by the quantum Ising system. The third stroke (C→D) (isothermal again where the field decreases) induces the heat released to the heat sink. The work done by the engine is basically the difference in heat absorbed and heat released. The engine efficiency has been calculated (as the ratio of work done and the heat absorbed by the engine) using the internal energy changes during these two strokes.

Last but not the least, the study of such dynamical behavior of the quantum heat engines using nonintegrable many-body condensed matter systems [10] (even with mean field approximation) are expected to be interesting and useful. The nonintegrable mean field equations here are simple (even compared to that of the quantum Heisenberg equation of motion for its unitary evolution). Moreover, the solutions of these nonlinear and nonintegrable mean field equations can provide the analysis of some instabilities at appropriate parameter values (of temperature, longitudinal field and transverse field) and give the crossover indications from its (quantum) heat engine to refrigerating engine behavior (even perhaps through supercritical pitchfork bifurcation [26]). It would also be interesting to study if such bifurcations are indeed there and can be observed. This would of course require considerably increased accuracy in the numerical solutions of the nonlinear dynamical equations for the quantum phase transition in the presence of the noncommuting time-dependent transverse field (see discussions in subsection IV.b).

Acknowledgements: Amit Dutta wanted us to explore the application of quantum mean field equation we had studied earlier in the context of dynamic hysteresis in quantum Ising systems to quantum Ising heat engines. He promised to teach us about the development and literature on quantum heat engines. We missed that opportunity because of his very sudden and untimely demise. We are thankful to Heiko Rieger and Eduardo Hernandez, former and present Editor-in-Chief of European Physical Journal B (EPJB), for taking the initiative of this Topical Issue on “Quantum phase transitions and open quantum systems: A tribute to Prof. Amit Dutta”, in memory of their one long time Editor. We would like to thank the Guest Editors of this Special Issue of EPJB, Uma Divakaran, Ferenc Iglói, Victor Mukherjee and Krishnendu Sengupta for kind invitation to contribute in it. We are extremely thankful to Victor Mukherjee for a careful reading of the paper and giving important suggestions. We are indebted to an anonymous referee for suggesting an extended study of the quantum Ising engine under external field. MA is grateful to the Presidency University for the FRPDF grant and BKC is grateful to the Indian National Science Academy for their Senior Scientist Research Grant.

Conflict of interest statement: We declare that this manuscript is free from any conflict of interest. The authors have no financial or proprietary interests in any material discussed in this article.

Data availability statement: The data may be available on request to the corresponding author.

Funding statement: No funding was received particularly to support this work.

Authors’ contributions: Bikas K. Chakrabarti-conceptualized the problem, analysed the results, developed the approximate analytic formulations, wrote the manuscript. Mukdish Acharyya-developed the code for numerical simulation, collected the data, prepared the figures, analysed the results, wrote the manuscript.

References

- [1] M. Acharyya, B. K. Chakrabarti and R. B. Stinchcombe, Hysteresis in Ising model in transverse field, *J. Phys. A: Math. Gen.* **27** 1533 (1994).
- [2] M. Acharyya and B. K. Chakrabarti, Response of Ising systems to oscillating and pulsed fields: Hysteresis, ac, and pulse susceptibility, *Phys. Rev. B* **52**, 6550 (1995)
- [3] H. E. D. Scovil and E. O. Schulz-DuBois, Three-Level Masers as Heat Engines, *Phys. Rev. Lett.* **2**, 262 (1959)
- [4] R. Alicki, The quantum open system as a model of the heat engine, *J. Phys. A: Math. Gen.* **12** L103 (1979)
- [5] T. Feldmann and R. Kosloff, Quantum four-stroke heat engine: Thermodynamic observables in a model with intrinsic friction, *Phys. Rev. E*, **68**, 016101 (2003)
- [6] T. Feldmann and Ronnie Kosloff, Quantum lubrication: Suppression of friction in a first-principles four-stroke heat engine, *Phys. Rev. E* **73**, 025107R (2006)
- [7] D. Gelbwaser-Klimovsky, R. Alicki and G. Kurizki, Minimal universal quantum heat machine, *Phys. Rev. E* **87**, 012140 (2013)

- [8] R. Alicki and M. Fannes, Entanglement boost for extractable work from ensembles of quantum batteries, *Phys. Rev. E* **87**, 042123 (2013).
- [9] R. Kosloff and Y. Rezek, The Quantum Harmonic Otto Cycle, *Entropy*, **19**, 136 (2017).
- [10] V. Mukherjee and U. Divakaran, Many-body quantum thermal machines, *J. Phys.: Condens. Matter*, **33** 454001 (2021).
- [11] S. Bhattacharjee and A. Dutta, Quantum thermal machines and batteries, *Eur. Phys. J. B* **94**, 239 (2021).
- [12] L. M. Cangemi, C. Bhadra and A. Levy, Quantum Engines and Refrigerators, arXiv: 2302.00726 (2023)
- [13] B. K. Chakrabarti, A. Dutta and P. Sen, Quantum Ising Phases and Transitions in Transverse Ising Models, Springer-Verlag, Heidelberg (1996)
- [14] A. Dutta, G. Aeppli, B. K. Chakrabarti, U. Divakaran, T. F. Rosenbaum and D. Sen, Quantum Phase Transitions in Transverse Field Spin Models: From Statistical Physics to Quantum Information, Cambridge University Press, Cambridge (2015)
- [15] S. K. Sarkar and D. Bose, Attractor for the mean-field equations of the hysteretic dynamics of a quantum spin model: Analytical solution, *Phys. Rev. E*, **55**, 2013 (1997)
- [16] L. B. Oftelie, S. Gulania, C. Powers, R. Li, T. Linker, K. Liu, T. K. S. Kumar, R. K. Kalia, A. Nakano and P. Vashishta, Domain-specific compilers for dynamic simulations of quantum materials on quantum computers, *Quantum Science and Technology*, **6**, 014007 (2020)
- [17] L. B. Oftelie, R. Van Beeumen, E. Younis , E. Smith, C. Iancu and W. A. de Jong, Constant-depth circuits for dynamic simulations of materials on quantum computers, *Materials Theory, Springer Open* **6**, 13 (2022)
- [18] G. Piccitto, M. Campisi and D. Rossini, The Ising critical quantum Otto engine, *New J. Phys.* **24**, 103023 (2023)
- [19] M. Suzuki and R. Kubo, Dynamics of the Ising Model near the Critical Point. I, *J. Phys. Soc. Japan* **24** 51 (1968)
- [20] P. M. Chaikin and T. C. Lubensky, Principles of condensed matter physics, Cambridge University Press, (1998)
- [21] H. E. Stanley, Introduction to phase transition and critical phenomena, Clarendon Press, Oxford, (1974)
- [22] B. K. Chakrabarti and M. Acharyya, Dynamic Transitions and Hysteresis, *Rev. Mod. Phys.* **71**, 847 (1999)
- [23] P. L. Krapivsky, S. Redner, E. Ben-Naim, A Kinetic View of Statistical Physics, Cambridge University Press, Cambridge (2010)
- [24] P. G. de Gennes, Collective motions of hydrogen bonds, *Sol. St. Commun.*, **1**, 132 (1963)

- [25] J. B. Scarborough, Numerical Mathematical Analysis, Oxford University Press, Oxford (1930).
- [26] S. H. Strogatz, Nonlinear dynamics and chaos, Westview press, USA (2004)